Spectroscopy of atomic hydrogen in dense plasmas in the presence of dynamic fields: Intra-Stark spectroscopy

E. A. Oks,* St. Böddeker, and H.-J. Kunze
Institut für Experimentalphysik V, Ruhr-Universität, 4630 Bochum, Federal Republic of Germany
(Received 18 April 1991)

The Lyman-α profile of hydrogen was studied in a gas-linear pinch, the plasma parameters of which were determined by Thomson scattering. The profiles displayed pronounced first- and second-order dips. The theory of dips in profiles of hydrogenlike spectral lines in plasmas containing quasimonochromatic electric fields, e.g., plasma waves or microwaves, is therefore further developed for high-density plasmas. The central point is the allowance of a spatial nonuniformity of the ion microfield that becomes more important with increasing density. Three qualitatively new features of the "dip" effect arise: (1) a significant shift of the dip positions (mostly to the blue side), (2) an appearance of dips in profiles of the central Stark components, and (3) an appearance of higher-order dips due to multiquantum resonances (between plasma waves and quasistatic Stark splitting). The measured blueshifts of the first- and the second-order dips are in fairly good agreement with the predictions of the present theory. This shift is much larger than the shift of the spectral line as a whole. The amplitude of the plasma waves as estimated from the measured half-widths of the dips was of the order of 2 MV/cm.

PACS number(s): 32.70.Jz, 52.70.Kz, 52.25.Rv

I. INTRODUCTION

The term "intra-Stark spectroscopy" is used to describe a set of resonant phenomena in spectral line profiles that becomes effective when a radiating atom (or ion) interacts simultaneously with a static electric field $\mathbf{F}$ and a quasimonochromatic electric field $\mathbf{E}(t)=\sum_j \mathbf{E}_j \cos(\omega t+\varphi_j)$. The static (or, more precisely, quasistatic) electric field $\mathbf{F}$ represents low-frequency plasma turbulence and/or ion microfields. It is characterized by some field-strength distribution $W(\mathbf{F})$ which reflects the fact that each radiator in a plasma experiences its "individual" quasistatic field $\mathbf{F}$. So in the absence of a quasimonochromatic electric field one observes a smooth quasistatic profile of a line corresponding to a smooth change in $\mathbf{F}$ from one radiator to another. The quasimonochromatic electric field $\mathbf{E}$ may represent Langmuir oscillations at a frequency $\omega \approx \omega_p = (4\pi e^2 N_e/m_e)^{1/2}$, where N_e is the electron density, or some other (e.g., lower-hybrid) waves developed in the plasma in such a way that their characteristic frequency ω is much greater than a characterstic width $\delta\omega$ of their frequency band. The quasimonochromatic electric field may represent as well some laser or microwave radiation at a frequency $\omega > \omega_p$, which penetrates into the plasma from the outside or is generated within the plasma. In any case, it is essential that in the presence of such fields some local peculiarities arise within the quasistatic Stark profile: dips or depressions at definite separations $\Delta\lambda^{\rm dip}$ from the line center λ_0.

The theory of the dip effect was developed in a set of papers [1–4], the last one containing the most detailed and up-to-date description. Therefore, we need not reproduce here the main theoretical points. It is only worthwhile mentioning that intra-Stark spectroscopy has some restricted physical analogy with the well-known intra-Doppler spectroscopy. In the latter, nonlinear optics phenomena manifest themselves as local peculiarities within a Doppler profile of a spectral line. A distinctive feature of intra-Stark spectroscopy is that one is dealing with a nonlinear dynamic-resonance effect of essentially multifrequency nature although the applied dynamic electric field is quasimonochromatic [3,4].

In various plasma experiments [1,2,5–7] dips or depressions in hydrogen spectral line profiles were reliably identified with theoretically predicted ones and were successfully used for the measurement of parameters of quasimonochromatic electric fields and of plasmas. Moreover in some other experiments [8–10] in which fine details of hydrogen or hydrogenlike line profiles were not analyzed by their authors, observed peculiarities could be also identified with theoretically predicted dips, as was pointed out in Refs. [1,11,12].

In some of these experiments [5–7,10], the electron density was very high: $N_e \geq 10^{18}$ cm^{-3}. At such densities, the electric field of thermally excited longitudinal plasma waves, $E^{\rm th}=[T/(e\pi r_D)]^{1/2}$, already reaches $\geq 10\%$ of the mean ion microfield $\langle F\rangle \approx 8.8eN_e^{2/3}$ as was pointed out in Ref. [5] with a numerical example of $E^{\rm th}\approx 0.11$ MV/cm and $\langle F\rangle \approx 1.3$ MV/cm for $N_e \approx 10^{18}$ cm^{-3} and $T_e \approx T_i \approx 10$ eV. This means that a relatively small increase of wave fields over the thermal level (which would not be a surprise for pulsed discharges) could lead to quasimonochromatic fields of the order of or greater than the mean ion microfield.

Even more important is another distinct feature of high-density plasmas. In the preceding theoretical calculations [1–4] the quasistatic electric field was considered

to be uniform. Let us assume now that the low-frequency plasma turbulence is absent or has a characteristic field strength $F_{\text{turb}} \ll 8.8eN_e^{2/3}$, so that the quasistatic field is represented mainly by the ion microfield. In high-density plasmas the spatial nonuniformity of the microfield becomes essential. This means that a dipole approximation is no longer sufficient for describing the interaction of a radiator with the perturbing ions, and higher multipoles (at least a quadrupole term) have to be taken into account.

In the following, therefore, we develop first the theory of the dip effect for dense plasmas. Three qualitatively new features appear at high densities: (1) a significant shift of the dip positions (mostly to the blue wing), (2) dips in the profile of the central Stark components, and (3) multiple-quantum-resonance dips. The experimental investigations of the Lyman-α profile of hydrogen as emitted by a gas-liner pinch are dealt with in Sec. III to be followed by a discussion of the results and conclusions in Sec IV.

II. THEORY OF THE DIP EFFECT FOR HIGH DENSITY PLASMAS

(i) We consider a radiative transition between levels of principal quantum numbers n and $n' < n$ of a hydrogenlike ion with a nuclear charge Z_r in a quasistatic electric field $\mathbf{F}$ and in a single mode $\mathbf{E}_0\cos\omega t$ of a quasimonochromatic field. The results can be easily extended to the case of multimode fields $\mathbf{E}=\sum_j \mathbf{E}_j\cos(\omega t+\varphi_j)$. It is sufficient to average the corresponding results for the single-mode case over a Rayleigh distribution $W_R(E_0,\bar{E})$ of the amplitudes E_0, where

$$W_R(E_0,\bar{E})=(E_0/\bar{E}^2)\exp[-E_0^2/(2\bar{E}^2)] ,$$
$$\bar{E}\equiv\left[\sum_j E_j^2/2\right]^{1/2} . \tag{1}$$

In the dipole approximation under the action of the electric field $\mathbf{F}$, the levels of a radiator with principal quantum numbers n and n' split into $(2n-1)$ and $(2n'-1)$ equidistant Stark sublevels separated from each other (in frequency units) by $\omega_F(n)=3n\hbar F/2Z_r m_e e$ and $\omega_F(n')$, correspondingly. The ensemble of radiators yields some distribution $W(F)$ of the absolute values of F. If the quasistatic Stark splitting of the upper level $\omega_{F*}(n)$ satisfies the condition of resonance with the monochromatic field for some groups of radiators at the electric field F^*, we may write

$$3n\hbar F^*/2Z_r m_e e \approx k\omega , \tag{2}$$

where $k=1,2,3,\ldots$ is the number of quanta of the field involved in the resonance. Because of this resonance, local peculiarities (dips or depressions) appear in the quasistatic profile $I_{\alpha\beta}(\Delta\omega)$ of each lateral Stark component [4] $\alpha\equiv(n,q,m)$, $\beta\equiv(n',q',m')$, $q=n_1-n_2$, and $q'=n_1'-n_2'$, where n_1,n_2,m and n_1',n_2',m' are the parabolic quantum numbers of the upper and lower Stark sublevels, respectively. The positions of these dips $\Delta\omega_\alpha^{\text{dip}}(k)$ are given by a simple relation [4]:

$$\Delta\omega_\alpha^{\text{dip}}(k)=3(nq-n'q')\hbar F^*/2Z_r m_e e$$
$$=n^{-1}(nq-n'q')k\omega . \tag{3}$$

For some other group of radiators, the quasistatic Stark splitting of the lower level $\omega_{F'*}(n')$ may also satisfy a condition analogous to Eq. (2), which leads to the appearance of a second set of dips in the profile $I_{\alpha\beta}(\Delta\omega)$ at the corresponding positions $\Delta\omega_\beta^{\text{dip}}(k)$ [4].

It should be emphasized that for relatively weak oscillating fields $E_0 \ll F^*$ (say, $E_0/F^* < 10^{-1}$) only the "first-order dips" arising from one-quantum resonances ($k=1$) can be observed [4]. As a consequence, only two dips [at $\Delta\omega_\alpha^{\text{dip}}(1)$ and $\Delta\omega_\beta^{\text{dip}}(1)$] will appear in the profile of each lateral Stark component. Naturally, for Lyman lines there is only one dip in the profile of each lateral Stark component [at $\Delta\omega_\alpha^{\text{dip}}(1)$] since the lower level ($n'=1$) has no quasistatic Stark splitting.

(ii) We now consider this effect in a high-density plasma and assume that low-frequency plasma turbulence is absent or its characteristic field strength F_{turb} is sufficiently low, i.e., $F_{\text{turb}} \ll F^*$. In this case the quasistatic fields involved in the resonances are caused mainly by the ion microfield. For dense plasmas one has to allow for a spatial nonuniformity of the ion microfield.

We include, therefore, into our considerations the quadrupole interaction of the radiator with the perturbing ions and treat the situation in the binary approximation in which only the nearest-neighbor perturber is taken into account. We point out that for lines from highly excited levels ($n \gg 1$) the influence of the ion microfield nonuniformity on dips might become essential already at lower densities. For this case, one can easily generalize the following results using a multiparticle description of the radiator-perturber quadrupole interaction in a way similar to Ref. [13], where such an approach was used for an investigation of the asymmetry of spectral lines.

Under the action of a perturbing ion (having a charge Z_p) at a distance R, the separation $\delta\omega_\alpha^+$ between the neighboring Stark sublevels α and $\alpha+1$ (see Fig. 1) may be expressed by (in frequency units) [14]

$$\delta\omega_\alpha^+=\delta a r^{-2}+\delta b_\alpha^+ r^{-3} , \tag{4}$$

where

$$r\equiv R/R_0 , \quad R_0\equiv(3Z_p/4\pi N_e)^{1/3} ,$$
$$\delta a\equiv(2Z_r m_e R_0^2)^{-1}3n\hbar Z_p , \tag{5}$$
$$\delta b_\alpha^+\equiv-(Z_r^2 m_e^2 e^2 R_0^3)^{-1}3Z_p\hbar^3 n^2(2q+1) ,$$

and where it was taken into account that the sublevel $\alpha+1$ has an electric quantum number $q+1$

In the case of a resonance of the oscillating field with Stark sublevels $\alpha,\alpha+1$, we have [instead of (2)]

$$\delta a r^{-2}+\delta b_\alpha^+ r^{-3}=k\omega . \tag{6}$$

Then the position of dips $\Delta\omega_{\alpha+}^{\text{dip}}(k)$ in the profile $I_{\alpha\beta}(\Delta\omega)$ of the same lateral Stark component is [instead of (2)]

$$\Delta\omega_{\alpha+}^{\text{dip}}(k)\approx n^{-1}(nq-n'q')k\omega$$
$$+2^{1/2}(27n^3 Z_r Z_p\omega_a)^{-1/2}(k\omega)^{3/2}u_\alpha^+ , \tag{7}$$

$$u_\alpha^+ \equiv n^2(n^2-6q^2-1)+6n(2q+1)(nq-n'q') -(n')^2[(n')^2-6(q')^2-1] ,$$
$$\omega_a \equiv me^4\hbar^{-3} \approx 4.14\times 10^{16}\mathrm{s}^{-1} \quad (8)$$

(ω_a is the so-called "atomic frequency").

A separation $\Delta\omega_a^-$ between Stark sublevels α and $\alpha-1$ (see Fig. 1) differs from $\Delta\omega_\alpha^+$ (in distinction from the pure dipole approximation):

$$\Delta\omega_\alpha^- = \delta a r^{-2} + \delta b_\alpha^- r^{-3} ,$$
$$\delta b_\alpha^- \equiv -(Z_r^2 m_e^2 e^2 R_0^3)^{-1} 3 Z_p \hbar^3 n^2 (2q-1) . \quad (9)$$

Therefore the oscillating field resonates with sublevels $\alpha,\alpha-1$ at some other value of a reduced perturber-radiator distance r. This leads to the appearance of an additional set of dips in the profile $I_{\alpha\beta}(\Delta\omega)$ at the positions

$$\Delta\omega_{\alpha-}^{\mathrm{dip}}(k) \approx n^{-1}(nq-n'q')k\omega + 2^{1/2}(27n^3 Z_r Z_p \omega_a)^{-1/2}(k\omega)^{3/2} u_\alpha^- , \quad (10)$$

where

$$u_\alpha^- \equiv n^2(n^2-6q^2-1)+6n(2q-1)(nq-n'q') -(n')^2[(n')^2-6(q')^2-1] . \quad (11)$$

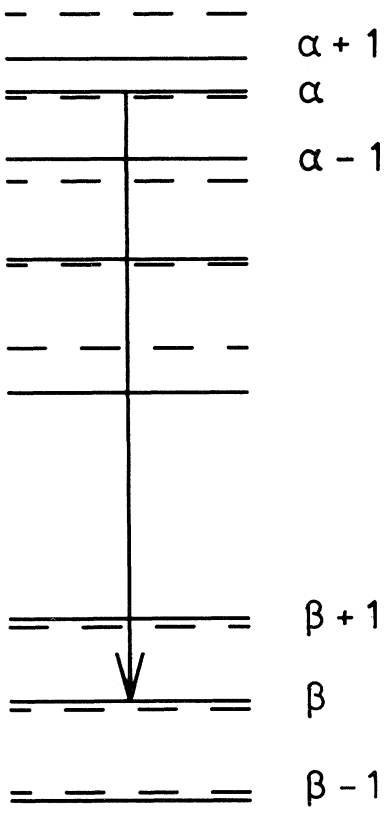

FIG. 1. Scheme of quasistatic Stark splitting of upper and lower levels in the ion microfield without (dashed lines) and with (solid lines) allowance for its nonuniformity. The radiative transition $\alpha\leftrightarrow\beta$ is indicated by an arrow.

Thus for a fixed number k of field quanta involved in a resonance, a "doublet dip" arises in the vicinity of the point $\Delta\omega_\alpha^{\mathrm{dip}}(k)=n^{-1}(nq-n'q')k\omega$ in the profile $I_{\alpha\beta}(\Delta\omega)$ of a *lateral* Stark component instead of a single dip. Both dips are significantly shifted (for most of the Stark components, the shift is to the blue wing).

Analogous qualitative changes occur in the vicinity of the points $\Delta\omega_\beta^{\mathrm{dip}}(k)=n'^{-1}(nq-n'q')k\omega$ in the profile $I_{\alpha\beta}(\Delta\omega)$ of the same lateral Stark component where dips due to a resonance of the oscillating field with a quasistatic Stark splitting of the lower multiplet would be located. Instead of this, now for each fixed number k two dips arise at the positions $\Delta\omega_{\beta\pm}^{\mathrm{dip}}(k)$ and $\Delta\omega_{\beta-}^{(k)}(k)$:

$$\Delta\omega_{\beta\pm}^{\mathrm{dip}}(k) = (n')^{-1}(nq-n'q')k\omega + 2^{1/2}[27(n')^3 Z_r Z_p \omega_a]^{-1/2}(k\omega)^{3/2} u_\beta^\pm , \quad (12)$$

where

$$u_\beta^\pm \equiv n^2(n^2-6q^2-1)+6n'(2q'\pm 1)(nq-n'q') -(n')^2[(n')^2-6(q')^2-1] . \quad (13)$$

(iii) We now consider consequences of the same resonances between a quasimonochromatic field and sublevels $\alpha,\alpha\pm1$ of the upper multiplet for the case in which the radiative transiton $\alpha\leftrightarrow\beta$ corresponds to a *central* Stark component of a spectral line. If a quadrupole perturber-radiator interaction were not taken into account, then the central component would be emitted at the position $\Delta\omega=0$ for all values r of a reduced perturber-radiator separation including the resonance value $r^*\approx(k\omega)^{-1/2}\delta a$. In this dipole approximation, perturbing ions do not produce so-called "inhomogeneous" Stark broadening in the vicinity of $\delta\omega=0$—nor if they are quasistatic or impact—and without inhomogeneous Stark broadening dips are not observable.

If we include a quadrupole perturber-radiator interaction, then at least in the wings of a central component perturbing ions can produce quasistatic (and, consequently, inhomogeneous) Stark broadening for dense plasmas, and resonances of the type (6) now lead to the appearance of dips in the profile $I_{\alpha\beta}(\delta\omega)$ of the central Stark component at the positions

$$\Delta\omega_\alpha^{c\,\mathrm{dip}}(k) = (b_\alpha - b_\beta) r^{*-3} \approx 2^{1/2}(27n^3 Z_r Z_p \omega_a)^{-1/2}(k\omega)^{3/2} u_c , \quad (14)$$

where

$$u_c \equiv n^2(n^2-6q^2-1)-(n')^2[(n')^2-6(q')^2-1] . \quad (15)$$

Analogously due to resonances between the quasimonochromatic electric field and sublevels $\beta,\beta\pm1$ of the lower multiplet, another set of dips are in the profile $I_{\alpha\beta}(\Delta\omega)$ of the same central Stark component at the positions

$$\Delta\omega_\beta^{c\,\mathrm{dip}}(k) \approx [27(n')^3 Z_r Z_p \omega_a]^{-1/2} 2^{1/2}(k\omega)^{3/2} u_c . \quad (16)$$

Thus, for each fixed number k of quanta involved in a resonance, a "doublet dip" arises in the central Stark component profile $I_{\alpha\beta}(\Delta\omega)$ as well as in the lateral Stark components. For central components this pair of dips is

always located in the blue wing.

(iv) Figure 2(a) shows H_α as an example: a theoretical pattern of shifted and doublet dips for the case of a relatively weak field ($E_0/F^* < 10^{-1}$) is displayed in which only first-order dips ($k=1$) are present. Dips in the far wings $|\Delta\lambda^{\rm dip}/\lambda_\omega| \geq \frac{4}{3}$ are not shown since they should be less pronounced (here and below $\lambda_\omega \equiv \omega\lambda_0^2/2\pi c$, where λ_0 is the unperturbed wavelength of the spectral line).

It is interesting to compare these theoretical predictions with depressions in the experimental profile of the H_α line obtained from a z-pinch discharge [5] (see Fig. 3). However, prior to any comparison with an experiment the question has to be addressed, from which "zero" point in a line profile the positions of the dips have to be taken since in dense plasmas a line profile as a whole experiences a shift $\Delta\lambda_{\rm sh}$. For neutral radiators, this total shift consists of a shift $\Delta\lambda_{\rm sh}^{(e)}$ produced by electrons [15,16] and of a quadrupole shift $\Delta\lambda_{\rm sh}^{(i)}$ produced by ions [13], the effect of changing matrix elements and hence changing intensities of the individual Stark components being included. The latter effect has the same origin as the shift of the dip positions and was therefore included into the resulting formulas (9), (10), (12), and (14). The electron shift $\Delta\lambda_{\rm sh}^{(e)}$, on the other hand, has to be taken into account in addition. In other words, dip positions must be read not from an unperturbed wavelength of a spectral line but from the point $\Delta\lambda_{\rm sh}^{(e)}$. For the case of the H_α profile of Ref. [5], this position corresponds to the experimentally observed shift, since theoretical calculations [17] show that the ion quadrupole shift is smaller than the electron shift by an order of magnitude and hence may be neglected. $\Delta\lambda = 9$ Å was observed for $N_e \approx 2\times10^{18}$ cm^{-3}.

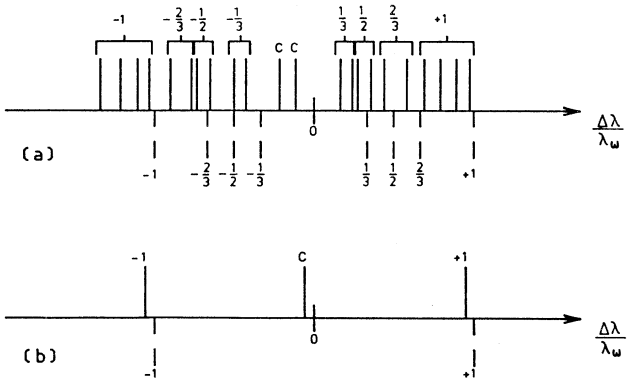

FIG. 2. Calculated positions of first-order dips in hydrogen lines profiles with allowance for a nonuniformity of the ion microfield (solid lines above abscissa axis). Dip positions without allowance for a nonuniformity of the ion microfield are shown by dashed lines below the abscissa with numbers indicating the separation of a dip from the unperturbed wavelength λ_0 in units $\lambda_\omega = \omega\lambda_0^2/2\pi c$, where ω is the frequency of a monochromatic electric field. The same numbers above the abscissa are used simply as labels which allow us to follow the correspondence between dip positions including the ion quadrupole shift and dip positions (below abscissa) without this shift. Positions of dips in the profile of the central Stark component are labeled c. (a) H_α line with $\omega = 5.6\times10^{13}$s^{-1} (or $N_e = 10^{18}$ cm^{-3}, if $\omega=\omega_p$), dips in the far wings $|\Delta\lambda^{\rm dip}/\lambda_\omega| \geq \frac{4}{3}$ are not shown: (b) L_α line with $\omega = 8.9\times10^{13}$ s^{-1} (or $N_e = 2.5\times10^{18}$ cm^{-3}, if $\omega=\omega_p$).

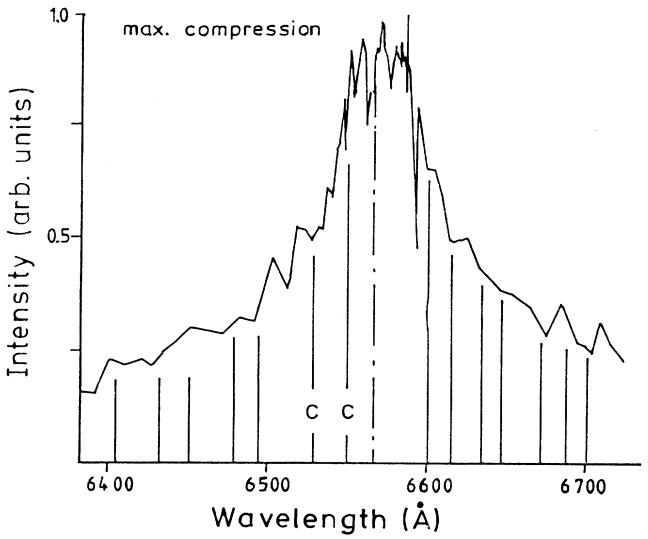

FIG. 3. Experimental profile of the H_α line from Ref [5]. The profile was recorded at the time of maximum compression of a z pinch i.e., for $N_e \approx 2\times10^{18}$ cm^{-3} and $T_e \approx 4$ eV. Vertical lines indicate the theoretically expected positions of dips calculated with allowance for a nonuniformity of the ion microfield according to the present paper. c denotes the expected positions of dips in the profile of the central Stark component.

The resulting theoretical positions of dips in the H_α profile are shown in Fig. 3 for $\omega \cong \omega_p$, where ω_p is the plasma frequency. There is a rather good agreement between the positions of experimentally observed depressions and theoretically calculated dips. It is worthwhile emphasizing that the discussed experimental H_α profile [5] seems to be the first in which the central component dips can be identified.

The simplest hydrogenlike line is Lyman-α. Naturally, the profile of L_α has also the simplest theoretical pattern of dips. For a fixed number k of quanta involved in a resonance one might observe three dips in the L_α profile: one dip in the profile of each Stark component (including the central component). All these dips of kth order are shifted to the blue side (compared to the points $\Delta\lambda = -k\lambda_\omega, 0, +k\lambda_\omega$) by the same value of $\delta\lambda(k)$,

$$\delta\lambda(k) = (3\omega_a)^{-1/2} 2(k\omega)^{3/2}\lambda_0^2/2\pi c \ . \tag{17}$$

For the case of $\omega=\omega_p$, Eq. (17) may be written as,

$$\delta\lambda\ (\text{Å}) \approx 5.97\times10^{-15} k^{3/2} N_e^{3/4} \ . \tag{18}$$

N_e is in cm^{-3}. The theoretical pattern of first-order dips ($k=1$) in the profile is shown in Fig. 2(b).

Dips of higher order ($k>1$) were not observed experimentally up to now. Even if the necessary condition $E_0/F > 10^{-1}$ is fulfilled, it is very difficult to identify reliably higher-order dips since for most hydrogenlike spec-

tral lines the theoretical dip pattern is rather complicated, and dips of different orders may be partially superimposed. From a theoretical point of view the best choice for an observation of higher-order dips is indeed the Lyman-α line.

III. EXPERIMENT

The investigation of the Lymann-α line of hydrogen was carried out employing the gas-liner pinch that has been described previously in the literature [18–20]. The gas-liner pinch acts as a modified z-pinch with a special gas inlet system. Two fast electromagnetic valves inject the so-called driver gas concentrically along the pinch wall and the test gas, whose spectral lines should be investigated, along the z axis into the vacuum vessel. After preionization and initiation of the main discharge the driver gas is accelerated into the center of the discharge chamber to form the plasma. The plasma parameters are nearly independent on the kind of test gas species because its amount is less than 1% of the driver gas. To prevent cooler outer layers of the test gas, the test gas is injected as late as possible. The plasma diameter is about 1.5 cm. The diameter of the discharge electrodes is 18 cm; their distance is 5 cm. The experimental settings are shown in Fig. 4.

For our investigations of L_α from hydrogen, both valves were filled with hydrogen. The main capacitor bank stored an energy of 3.5 kJ and the energy for preionization was about 10 J. The implosion time was 3.0 μs and the decay-time duration was 4.0 μs. The maximum electron density was 2.9×10^{18} cm^{-3} and the maximum electron temperature kT_e was 12.5 eV.

We redetermined the plasma parameters by coherent Thomson scattering as used in earlier studies [21]. The detector system consisted of a 1-m monochromator (SPEX No. 1704 with a 1200 lines/mm grating blazed at 5000 Å) and of an optical-multichannel-analyzer system (Spectrosccopy Instruments model IRY-700G) at the exit slit with 700 sensitive channels. The reciprocal dispersion of this system was 0.2 Å/ channel; the FWHM of the apparatus profile was 0.7 Å.

The observation system in the vacuum-uv region consisted of a 1-m normal-incidence spectrometer (McPherson model 225) with a concave grating of 1200 lines/mm, blazed at 1200 Å. The entrance slit was 25 μm. The exit slit was replaced by a CsI-coated microchannel plate of chevron type (Galileo model CEMA 3025). The visible light of the attached P20 phosphor screen was recorded with a second OMA system (EG&G model 1420). The total reciprocal dispersion for this system was 0.209 Å/channel. In first order the FWHM of the apparatus profile was 1.7 Å.

The exposure time was 30 ns and was determined by an approximately rectangular pulse to the MCP; this pulse was coupled with the triggering of the laser, and in this way the density measurement was at the same time as the spectroscopic observation. To suppress impurity lines in higher spectral order, especially lines from oxygen, a MgF_2 filter was mounted between pinch and vacuum-uv system, cutting off radiation below 1100 Å [21].

A comparison of spectra taken with and without this filter showed that indeed all oxygen lines in second order were removed from the L_α profile.

The radiation of the plasma column was monitored at 5200 Å by an $\frac{1}{4}$-m monochromator equipped with a RCA 1P28 photomultiplier; this monitor showed the reproducibility of the discharge and the time between maximum compression and observation.

For high-density and low-temperature plasmas ($N_e \leq 2.9\times10^{18}$ cm^{-3}, $kT_e \leq 12.5$ eV), we measured simultaneously the line shape of the Stark broadened L_α

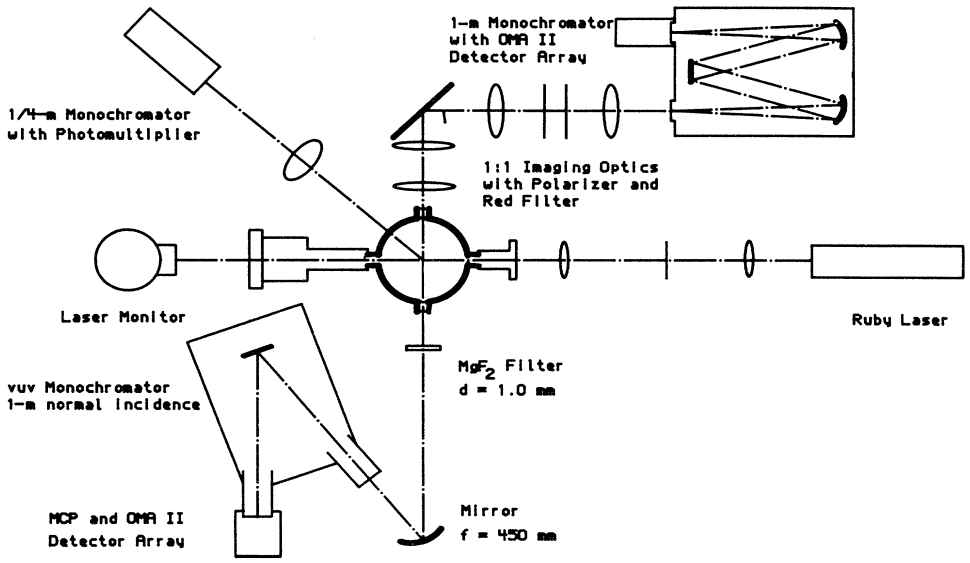

FIG. 4. Experimental setup. The diagnostic equipment consists of a ruby laser and three monochromators, two equipped with an OMA system. The positions of a photomultiplier and the laser monitor are also shown.

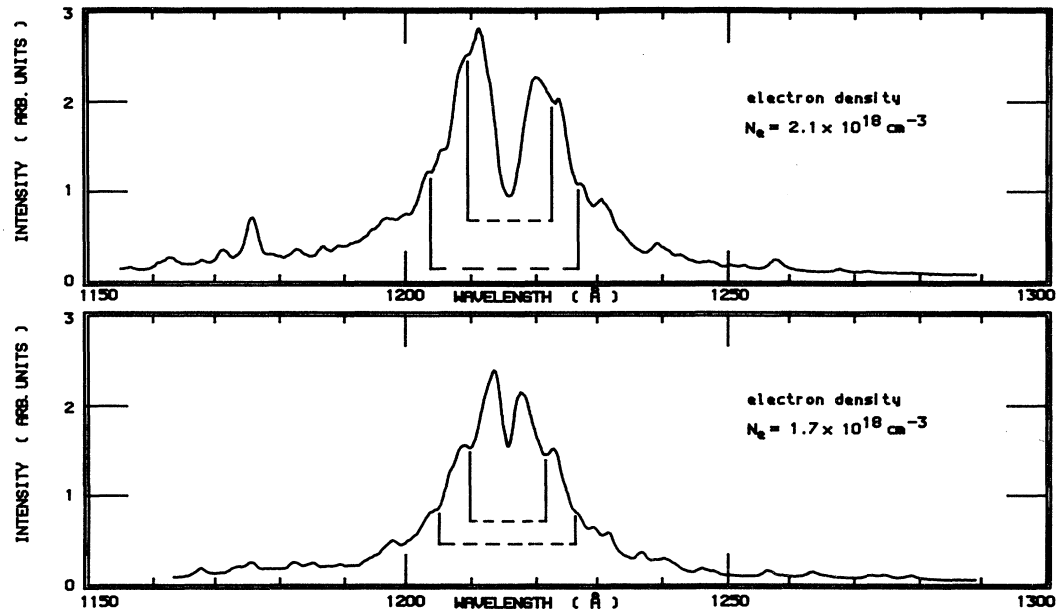

FIG. 5. Comparison of the experimental and the theoretical positions of dips in the L_α line profiles caused by a joint action of the dynamic electric field (Langmuir waves) and the quasistatic ion microfield. The spectra were taken 110 ns (top) and 200 ns (bottom) after maximum compression. Electron densities obtained by coherent Thomson scattering are also pointed out. Positions of first- and second-order dips, respectively, calculated according to the present theory, are denoted by the pairs of vertical solid lines connected by a dashed line.

line of hydrogen and the scattered light from coherent Thomson scattering to determine the density and the temperature of our plasma. Figure 5 shows two line profiles that were taken (a) 110 ns and (b) 200 ns after maximum compression. As predicted by theory, all profiles show dips; they are marked. For the analysis of the dip positions, the spectra were evaluated with higher precision than in the picture by simply extending the wavelength scale and viewing the respective part of the line profile. Figure 6 shows such a part of a line profile. The identification of dips posed no problem in most cases when looking for a pair or even two consistent pairs of

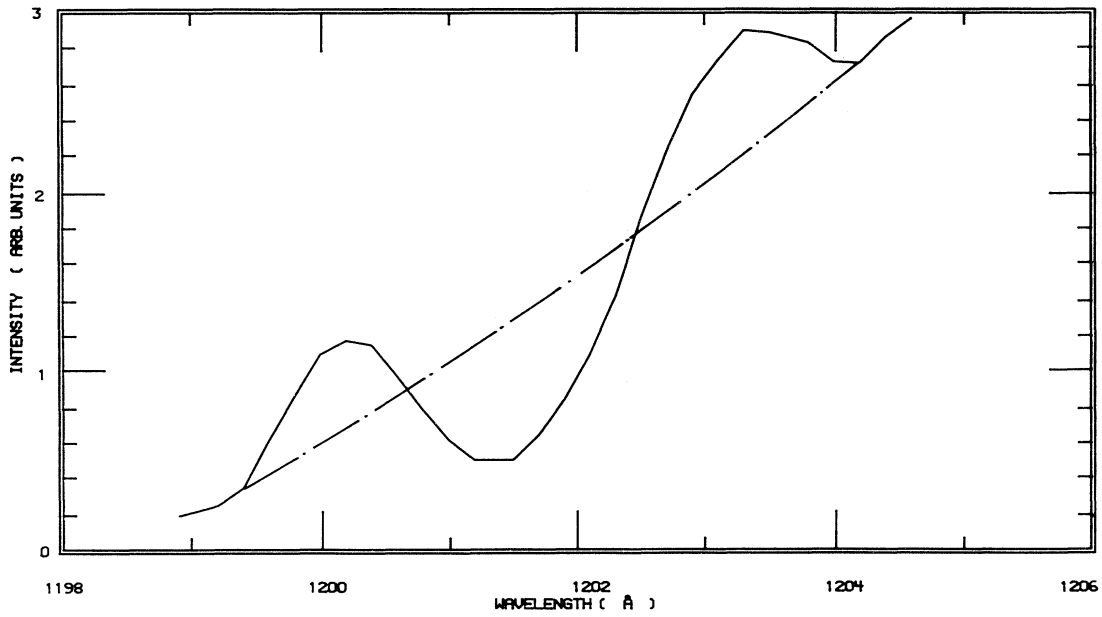

FIG. 6. Part of the line profile showing the dip and two adjacent bumps.

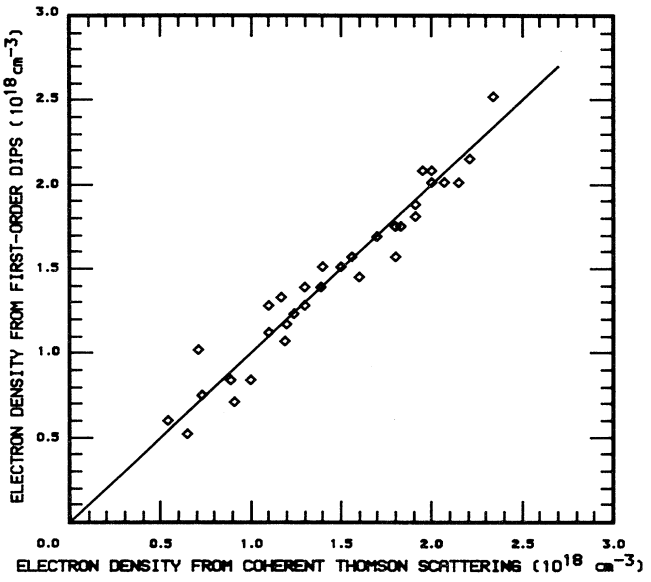

FIG. 7. Electron densities calculated from the separation of pairs of the first-order dips vs the electron density obtained by coherent Thomson scattering.

dips. Furthermore, dip positions have to change consistently during the discharge; impurity lines are at fixed wavelength positions in the quiescent phase of the plasma.

Figures 7 and 8 display the density derived from the separation of pairs of dips (assuming $\omega \cong \omega_p$) against the density taken from Thomson scattering. This evaluation eliminates uncertainties of the line center caused by uncertainties of the shifts. Higher than secord-order dips are not evaluated, because of impurity lines at their predicted positions and because of lower intensities at the line wings, both causing large uncertainties in finding the dips. Both figures show good agreement between the independently obtained densities over the whole range of measured density. In Fig. 9 one can see that the second-order dips are as reliable as the first-order dips for a determination of the electron density. The scatter of the data points around the solid line reflects the uncertainty of each dip position, which corresponds to ± 2 pixels, and a 10% uncertainty in the density from coherent Thomson scattering, respectively.

The structures on the L_α line are on both sides of the profile; they consist of dips of first and second order, every dip being accompanied by two bumps on each side of the dip. For lower electron densities and hence small Stark width the lower bumps from first-order dips are superposed with the upper bumps from second-order dips, so that there is only one bump instead of two.

Using again pairs of dips, we determined the shift of the dips once taking the position of the self-absorption dip as a reference position, and a second time from an absolute wavelength scale, which was derived from the position of impurity lines; we used the N V lines at 1238.82 and 1242.86 Å, and the C III multiplet at about 1175 Å ($^3P^0 - {}^3P$). Both give shifts which are consistent with the predictions. Figures 10 and 11 illustrate the results of the shift relative to the self-absorption dip.

At low densities the deviation is caused by the limited resolution of the vaccum-uv instrument; the shift is only about one and a half times the resolution per channel. At high densities the deviation is caused by the uncertainty of the absolute wavelength scale due to uncertainties in the determination of the peaks of the impurity lines; be-

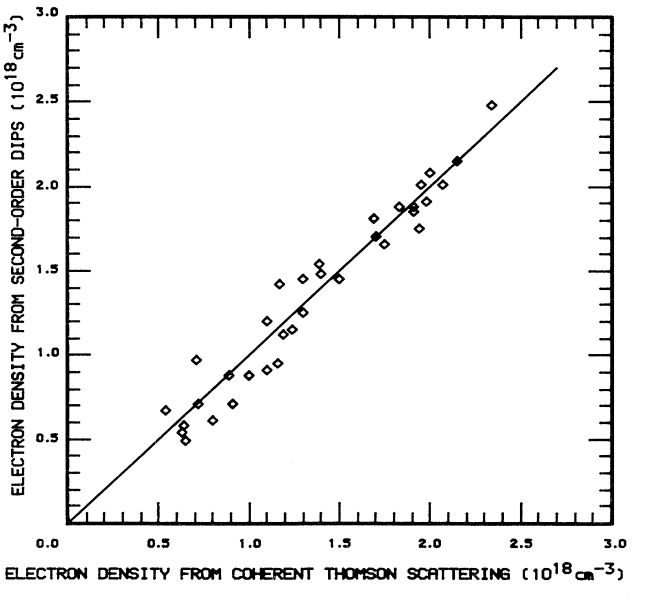

FIG. 8. Electron densities calculated from the separation of pairs of second-order dips vs the electron density obtained by coherent Thomson scattering.

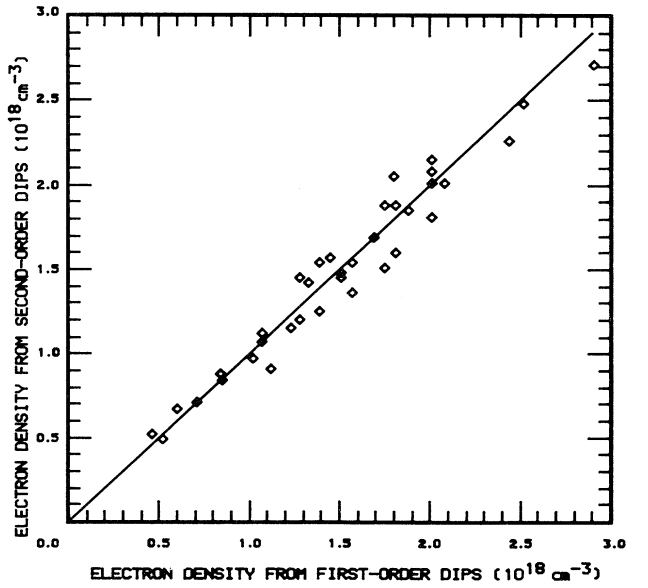

FIG. 9. Comparison of electron densities obtained from the first- and second-order dips.

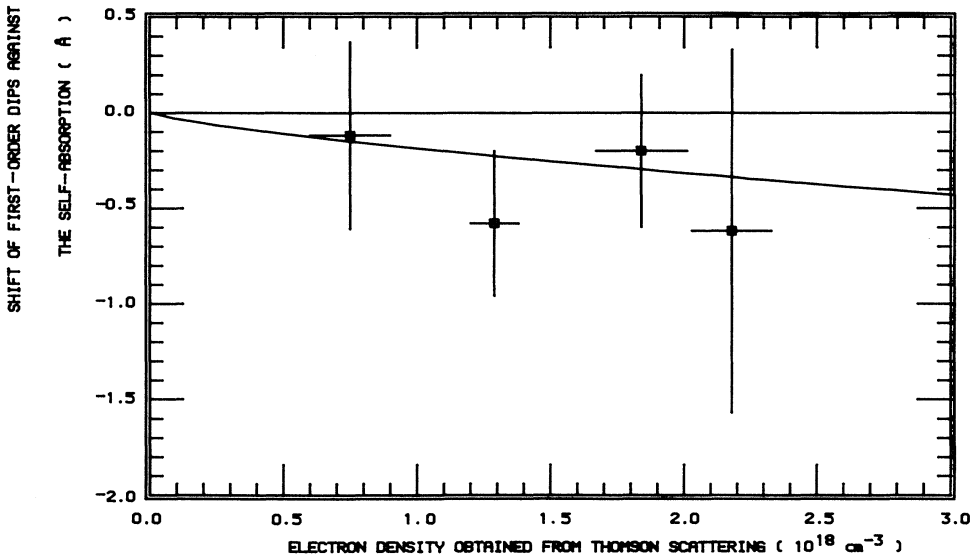

FIG. 10. Blueshift of the first-order dips against the line center vs the electron density obtained by the coherent Thomson scattering. The line center was determined from the point of lowest intensity in the center of the line profile (self-absorption dip). The solid curve shows the shift calculated according to the present theory.

cause of their low intensity the real line center was not always easy to fix. To prevent any influence of the impurities on the plasma parameters and on the line shape, we kept their concentration low.

When analyzing the shift against the dip of self-absorption caused by hydrogen atoms in a cold boundary, corrections are necessary because of the possible influence of a central dip. It might also be accompanied by two bumps and would be shifted, so that the deepest point in the line profile may not mark the unperturbed line center. The central part of the line profile has been formed by a cold outer layer of the plasma column with a different electron density and electron temperature. However, the central part does not influence the present results which were obtained from the line wings sufficiently away from the line center.

It can be seen that the theory describes the experimental findings qualitatively and within the experimental errors also quantitatively. With higher resolution in the vacuum-uv region the shifts could be determined more exactly.

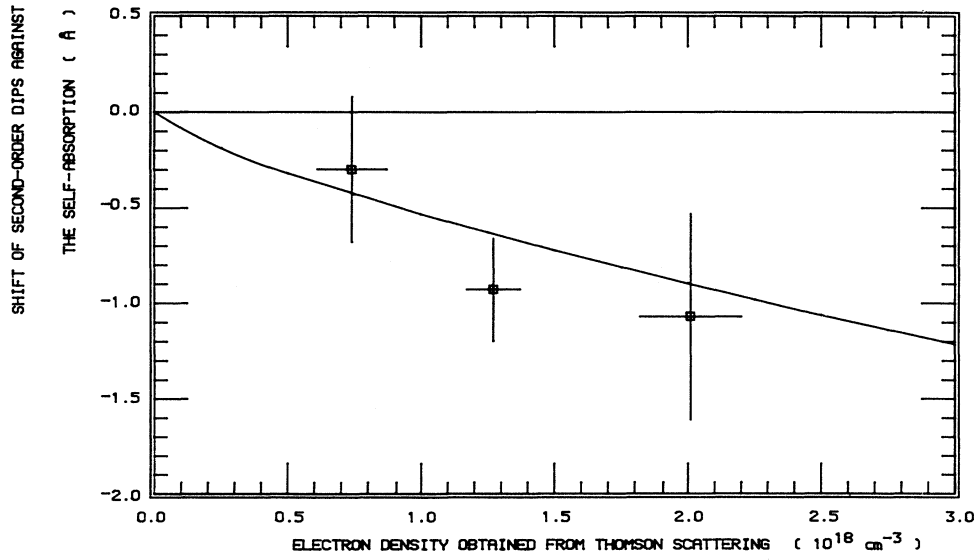

FIG. 11. The same as Fig. 10 but for the second-order dips.

IV. DISCUSSION AND CONCLUSIONS

The analysis of the entire set of data from the present experiment confirms the theoretical predictions for dips in spectral line profiles both qualitatively and quantitatively for high-density plasmas. The fact that dips in the central component profile were not observed (in distinction from our analysis of the experimental H_α profile displayed in Ref. [5]) has the following explanation: for most perturbing ions, the condition of local quasistaticity of the L_α *central* component profile at the dip position is not satisfied in the present experiment.

A rather good agreement of the "shifted-dips" theory with the experiments means, in particular, that the condition $F_{\rm turb} \ll F^*$ is indeed fulfilled. For our case of $\omega \cong \omega_p$, a practical formual for F^* has the form

$$F^*(\mathrm{V/cm}) \approx 2.34 \times 10^{-3} N_e^{1/2} . \quad (19)$$

For $N_e = 2.5 \times 10^{18}$ cm^{-3}, we obtain $F^* \approx 3.7$ MV/cm. (Note that at this density, a "resonance" value F^* of the ion microfield is more than five times larger than the Holtsmark normal field strength, $F_H \approx 2.60 e N_e^{2/3} \approx 0.7$ MV/cm.) Thus, low-frequency turbulent fields were either not developed in the present experiment or had strengths $F_0 \ll 4$ MV/cm.

For some of the experimental L_α profiles, the entire structure in the vicinity of the first-order dips is sufficiently resolved (see Fig. 6) that it is possible to determine experimentally a half-width $\delta\lambda_{1/2}^{\rm dip}$ of a dip (or an equal value of a distance between the dip minimum and the nearest bump): this allows us to estimate an amplitude E_0 of the quasimonochromatic field according to the following general formula for a half-width of a first-order dip [4]:

$$\Delta\lambda_{1/2}^{\rm dip} \approx (\tfrac{3}{2})^{1/2} \lambda_0^2 n^2 \hbar E_0 / 8\pi m_e e c , \quad (20)$$

where the field is assumed to have an isotropic distribution (over an ensemble of radiators). For the Lyman-α line ($n=2$), the corresponding practical formula has the form

$$E_0(\mathrm{V/cm}) \approx 1.3 \times 10^6 \Delta\lambda_{1/2}^{\rm dip} \quad (21)$$

with $\Delta\lambda_{1/2}^{\rm dip}$ in units of Å.

For a characteristic experimental value $\Delta\lambda_{1/2}^{\rm dip} \approx 1.5$ Å, this equation yields $E_0 \approx 2$ MV/cm. Thus we obtain a ratio $E_0/F^* \cong 0.5$ which is sufficiently high to explain the appearance of second-order dips in the profiles of the present experiment.

It is instructive to compare characteristic values of the shift of the dips with characteristic values of the shift of the spectral line as a whole. For neutral radiators the latter consists of the shift $\Delta\lambda_{\rm sh}^{(e)}$ produced by electrons [15,16] and of a quadrupole shift $\Delta\lambda_{\rm sh}^{(i)}$ produced by ions [13,17] (as was already mentioned). For higher temperatures, we estimate from Ref. [15]

$$\Delta\lambda_{\rm sh}^{(e)} \approx 7.5 \times 10^{-20} N_e . \quad (22)$$

For $N_e = 2.5 \times 10^{18}$ cm^{-3}, formula (22) gives a redshift $\Delta\lambda_{\rm sh}^{(e)} \approx 0.2$ Å. It should be emphasized that for high-density plasmas ($N_e \gtrsim 10^{18}$ cm^{-3}) the electron-produced shift $\Delta\lambda_{\rm sh}^{(e)}$ should be calculated with allowance for huge microfields $F \gtrsim 1$ MV/cm produced by the ions. This field mixes the degenerated states of a radiator (in terms of spherical quantization states used by Griem [15,17]), and this reduces the value of $\Delta\lambda_{\rm sh}^{(e)}$ as was shown in Ref. [23]. Furthermore, the main contribution to the shift is caused by $\Delta n \neq 0$ collisions and can be produced only by those electrons whose influence on the radiating atom may be described in the impact approximation. Since for an essential part of broad line wings (corresponding to large ion microfields) the impact approximation for the electron fails—partially for near wings and completely for far wings—the true electron-produced shift $\Delta\lambda_{\rm sh}^{(e)}$ should be further reduced compared to the calculations of Griem (Refs. [15] and [17]). Thus, the electron-produced shift is several times smaller than the shift of the first-order dip positions $\delta\lambda(1) \approx 0.38$ Å and one order of magnitude smaller than the shift of the second-order dip positions $\delta\lambda(2) \approx 1.06$ Å in the L_α profile at our density [see Eq. (17)].

The ion quadrupole shift $\Delta\lambda_{\rm sh}^{(i)}$ of the L_α line as a whole is of the same order as the ion quadrupole shift of its central component $\Delta\lambda_{{\rm sh},c}^{(i)}$. The latter may be well estimated by the binary approximation formula $\Delta\lambda_{{\rm sh},c}^{(i)} \approx -2[e^2/(\hbar c)]\lambda_0^2 a_0^2 N_e$ (a_0 is the Bohr radius), or from Ref. [17] we deduce

$$\Delta\lambda_{\rm sh}^{(i)}(\text{Å}) \approx -(1-2) \times 10^{-20} N_e . \quad (23)$$

For $N_e = 2.5 \times 10^{18}$ cm^{-3}, we obtain $\Delta\lambda_{{\rm sh},c}^{(i)} \approx -4 \times 10^{-2}$ Å. This value is about 10 and 25 times smaller than the (ion quadrupole) shifts of the first- and the second-order dip positions in the L_α profile, at this density, respectively.

Thus we arrive at the following conclusions. The dip effect in hydrogenlike line profiles acquires qualitatively new features in high-density plasmas due to the rising role of a spatial nonuniformity of the ion microfield. First, we have recorded a significant blueshift of dip positions compared to their positions calculated previously [1–4] in the dipole approximation. This shift is in good agreement with the predictions of the theory developed in the present paper, which takes into account a quadrupole contribution to a perturber-radiator interaction. It should be especially emphasized that the shift of the dip positions is much greater than the shifts of the spectral line as a whole [13–18] so that the former is a much more easily and reliably observable effect.

Second, an essential part of the profile of central Stark components is dominated by ion quasistatic broadening (through a quadrupole interaction). In this quasistatic part of the central component, profile dips may also be formed. The higher the principal quantum number of an upper level n is, the more favorable are conditions for observing such "central" dips although central components become relatively weaker for higher n. Our analysis of the experimental H_α profile from Ref. [5] clearly reveals the presence of the central dips. (In the L_α profiles from the present experiment, central dips are not so pronounced since only corresponding "bumps" surrounding

central dips are located in the quasistatic part of the central component profile; in addition, central dips themselves are suppressed by self-absorption).

Third, the higher the density, the greater the ratio E_0/F^* can be of a quasimonochromatic field and a resonance value of a quasistatic electric field. Therefore, multiquantum-resonance dips may become observable just as was the case for the two quantum resonance dips in our experiment.

Finally, the experimental determination of the distances between the dips or between the dips and the line center represents an easy and precise method for measuring the frequency of a quasimonochromatic field in a dense plasma. In particular, if the field corresponds to Langmuir waves, one has an additional method for the measurement of high electron densities N_e. The purity of the plasma must be high to prevent false interpretations of peculiarities in the profiles which are caused by impurity lines. The experimental determination of a dip halfwidth allows an estimate of the amplitude of the quasimonochromatic field as well.

Note added in proof. The idea of a resonant-type restructuring of spectral lines of a hydrogen atom subjected simultaneously to a static and a high-frequency field has been approached first by a numerical calculation [23].

ACKNOWLEDGMENTS

The work was supported by the Sonderforschungsbereich 191. E. A. O. was supported by the Alexander von Humboldt Foundation. The authors are grateful to Hans Griem for helpful discussions and comments.

*Present address: Department of Physics, 206 Allison Laboratory, Auburn University, Auburn, AL 36849-5311.

[1] A. I. Zhuzhunashvili and E. A. Oks, Zh. Eksp. Teor. Fiz. **73**, 2142 (1977) [Sov. Phys. JETP **46**, 1122 (1977)].

[2] E. A. Oks and V. A. Rantsev-Kartinov, Zh. Eksp. Teor. Fiz. **79**, 99 (1980) [Sov. Phys. JETP **52**, 50 (1980)].

[3] V. P. Gavrilenko and E. A. Oks, Zh. Eksp. Teor. Fiz. **80**, 2150 (1981) [Sov. Phys. JETP **53**, 1122 (1981)].

[4] V. P. Garilenko and E. A. Oks, Fiz. Plazm. **13**, 39 (1987) [Sov. Phys. J. Plasma Phys. **13**, 22 (1987)].

[5] K. H. Finken, R. Buchwald, G. Bertschinger, and H.-J. Kunze, Phys. Rev. A **21**, 200 (1980).

[6] K. H. Finken, Fortschr. Phys. **31**, 1 (1983).

[7] G. Bertschinger, Ph.D. thesis, Bochum University, 1980 (unpublished).

[8] C. C. Gallgher and M. A. Levine, Phys. Rev. Lett. **30**, 897 (1973).

[9] W. R. Rutgers and H. de Kluiver, Z. Naturforsch. **29a**, 42 (1974).

[10] B. Yaakobi, D. Steel, E. Thorsos, A. Hauer, and B. Perry, Phys. Rev. Lett. **39**, 1526 (1977).

[11] E. A. Oks, Meas. Techniques **29**, 805 (1986).

[12] E. A. Oks, in the *14th International Symposium on the Physics of Ionized Gases, Invited Lectures, Sarajewo, Yugoslavia, 1988,* edited by L. Tanović, N. Konjević, and N. Tanović (Nova Science, Commack, 1989), p. 435.

[13] A. V. Demura and G. V. Sholin, J. Quantum Spectrosc. Radiat. Trans. **15**, 881 (1975).

[14] G. V. Sholin, Opt. Spectrosc. **24**, 275 (1969).

[15] H. Greim, Phys. Rev. A **38**, 2943 (1988).

[16] D. B. Boerker and C. A. Iglesias, Phys. Rev. A **30**, 2771 (1984).

[17] H. R. Griem, Phys. Rev. A **28**, 1596 (1983).

[18] K. H. Finken and U. Ackermann, J. Phys. D **15**, 615 (1982).

[19] K. H. Finken and U. Ackermann, J. Phys. D **16**, 773 (1983).

[20] A. Gawron, S. Maurmann, F. Böttcher, A. Meckler, and H.-J. Kunze, Phys. Rev. A **38**, 4737 (1988).

[21] J. A. R. Samson, *Techniques of Vacuum Ultraviolet Spectroscopy* (Wiley, New York, 1967).

[22] A. Gawron, J. D. Hey, X. J. Xu, and H.-J. Kunze, Phys. Rev. A **40**, 7150 (1989).

[23] A. Cohn, P. Bakshi, and G. Kalman, Phys. Rev. Lett. **29**, 324 (1972).